JOC Article

Mechanism and Chemoselectivity of the Pd(II)-Catalyzed Allylation of Aldehydes: A Density Functional Theory Study

Fabio Pichierri[*,†] and Yoshinori Yamamoto[‡]

COE Laboratory, Tohoku University, IMRAM, 2-1-1 Katahira, Sendai 980-8577, Japan, and the Department of Chemistry, Graduate School of Science, Tohoku University, Sendai 980-8578, Japan

fabio@tagen.tohoku.ac.jp

Received September 27, 2006

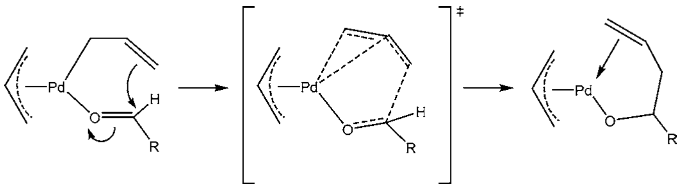

Density functional theory calculations at the PBE1PBE/DGDZVP level of theory were performed to investigate the mechanism and chemoselectivity of Pd(II)-catalyzed allylation of aldehydes. The transfer of formaldehyde to the π-allyl group of bis-π-allylpalladium complex is a thermodynamically favored process ($\Delta G = -1.4$ kcal/mol), and its Gibbs free energy of activation ($\Delta G^{\ddagger}$) corresponds to 23.0 kcal/mol. Further support for the mechanism proposed herein, which requires the coordination of an aldehyde molecule to the metal center, comes from correctly predicting the chemoselectivity of the reaction when it is conducted with mixed bis-π-allylpalladium complexes containing crotyl, methallyl, and 2-methoxyallyl groups.

Introduction

Homoallylic alcohols can be synthesized from the reaction between allylstannanes and aldehydes in the presence of Lewis acids either at high temperatures or at high pressures.[1] Yamamoto and co-workers[2] have shown, however, that homoallylic alcohols can be obtained in high yields at room temperature without using Lewis acids when the reaction is carried out in the presence of Pd(II) or Pt(II) complexes (eq 1). Furthermore, by using NMR spectroscopy, these authors have been able to identify the key intermediate of the Pd-catalyzed allylation of aldehydes (and imines), characterized as the bis-π-allylpalladium complex **1**, shown in eq 1. Most importantly, the symmetric bis-π-allylpalladium intermediate exhibits nucleophilic reactivity, in stark contrast with the electrophilic reactivity of ordinary π-allylpalladium complexes of type Pd(η^3-allyl)XL, with X = halogen, OAc, etc. and L = ligand (eq 2).[3] The latter complexes are generated from allyl halides, acetates, or related substrates in the presence of Pd(0). The resulting π-allylpalladium complexes do not react with aldehydes and imines since the π-allyl group of these complexes exhibits electrophilic reactivity.

CHART 1

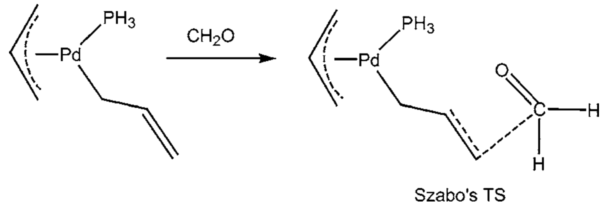

In a recent theoretical study based on density functional theory (DFT) calculations, Szabó[4] investigated the amphiphilic character of the title bis-π-allylpalladium complex **1** with the purpose of explaining the observed mechanistic differences of its reactivity toward nucleophiles and electrophiles. The electronic structure calculations indicated the presence of d−π hyperconjugative interactions in the η^1-allyl moiety of the (η^1-allyl)(η^3-allyl)Pd(PH_3) intermediate (Chart 1), which has been suggested to affect its structure and reactivity toward electrophiles and nucleophiles. Most importantly, the energy barrier associated

---

[†] COE Laboratory.

[‡] Graduate School of Science.

(1) For reviews, see: (a) Yamamoto, Y.; Asao, N. *Chem. Rev.* **1993**, *93*, 2207. (b) Marshall, J. A. *Chem. Rev.* **2000**, *100*, 3163. (c) Denmark, S. E.; Fu, J. *Chem. Rev.* **2003**, *103*, 2763.

(2) (a) Nakamura, H.; Iwama, H.; Yamamoto, Y. *J. Am. Chem. Soc.* **1996**, *118*, 6641. (b) Nakamura, H.; Bao, M.; Yamamoto, Y. *Angew. Chem., Int. Ed.* **2001**, *40*, 3208. (c) Marshall, J. A. *Chemtracts: Org. Chem.* **1997**, *10*, 40.

(3) For a recent review, see: Szabó, K. J. *Chem.−Eur. J.* **2004**, *10*, 5268.

(4) Szabó, K. J. *Chem.−Eur. J.* **2000**, *6*, 4413.

10.1021/jo061985r CCC: $37.00

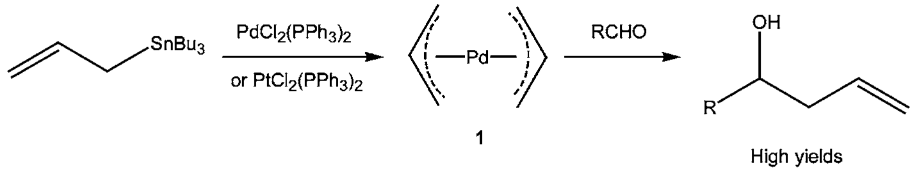

(1)

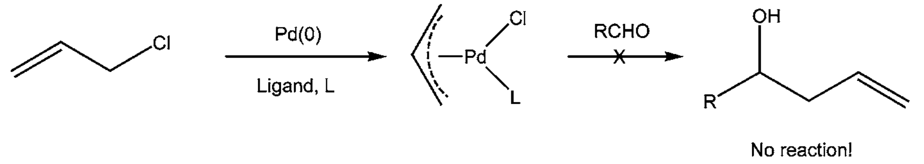

(2)

with the transition state (TS) arising from the intermolecular attack of one molecule of formaldehyde (CH_2O) on the η^1-allyl moiety of the Pd(II) precursor complex was estimated to be 4.3 kcal/mol (a value of 7.5 kcal/mol was computed by including the zero-point energy correction, ZPE).

According to the experimental findings of Yamamoto and co-workers, the presence or absence of phosphine can be exploited to control the chemoselective allylation of aldehydes (imines) to yield homoallylic alcohols (amines).[2b] While the coordination of phosphine to Pd(II) is essential for the Stille coupling reaction,[5] this is not the case for the allylation reaction whose mechanism (Chart 2) would rather involve an intermediate complex (**1-r**) in which the aldehyde is coordinated (via oxygen) to the metal center.[6] In the present computational study, we want to see whether the presence of phosphine is pertinent to the Pd-catalyzed allylation of aldehydes discovered by Yamamoto and co-workers. To do so, we employ modern DFT methods to characterize the structures and stabilities of the complexes **1-r** and **1-p**, which have a formaldehyde molecule coordinated to Pd(II), and the corresponding transition state (vide infra) that arises from the nucleophilic attack of the η^1-allyl moiety to the coordinated aldehyde of **1-r**. The subsequent transmetalation of **1-p** with allyltributyltin ($C_3H_5SnBu_3$) closes the catalytic cycle of Chart 2 by producing again **1** and homoallyloxystannane.[2b] Furthermore, we set out to investigate the chemoselectivity of the Pd(II)-catalyzed aldehyde allylation reaction that proceeds through the asymmetric bis-π-allylpalladium complexes **2**−**4** obtained by using crotyl-, methallyl-, and 2-methoxyallylstannanes (Chart 3). According to the original experiments of Yamamoto and co-workers, benzaldehyde was transferred on the coordinated π-allyl group of **2**, whereas for **3** and **4**, the transfer occurred on methallyl and 2-methoxyallyl groups, respectively.[2a]

Computational Details

All of the DFT calculations were performed with the Gaussian03 software package.[7] The PBE1PBE hybrid functional[8a] containing the generalized gradient functional of Perdew, Burke, and Ernzerhov (PBE)[8b,c] and a predefined amount of Hartree−Fock exchange energy was employed in combination with the all-electron double-ζ valence-polarized basis set of DGauss (DGDZVP).[9] Calculations using the Stuttgart−Dresden SDD basis set[10] for Pd (Pt) and using the DGDZVP basis set for the remaining elements were also carried out. SDD implements relativistic effective core potentials (ECPs), which replace the core electrons of nuclei below the second row, thereby reducing the computational cost of electronic structure calculations on molecules containing heavy elements. Transition-state (TS) structures were located by employing the synchronous transit-guided quasi-Newton (STQN) method of Schlegel and co-workers.[11] Accordingly, the search of an unknown TS structure is performed using the optimized structures of both reactant and product as input. Frequency calculations have been carried out for all of the optimized geometries to check that local minima are being characterized by real vibrational frequencies, while transition states are requested to possess only one imaginary frequency.[12] Atomic charges were computed with the natural population analysis (NPA) method of Weinhold and co-workers,[13] which overcomes some deficiencies encountered with the canonical Mulliken-type charges. The binding energy of selected complex species was computed while taking into account the well-known basis set superposition error (BSSE) by means of the counterpoise approximation method of Boys and Bernardi.[14] Pre- and postprocessing operations were carried out with the GaussView[15] (version 3.09) and Molden[16] (version 4.4) graphical interfaces.

---

(5) For a review of the Stille coupling reaction, see: Farina, V.; Krishnamurthy, V.; Scott, W. J. *Org. React.* **1997**, *50*, 1.

(6) A square-planar Pd(II) complex with benzaldehyde, PhCHO, coordinated to the metal center via the oxygen atom has been structurally characterized by single-crystal X-ray diffraction analysis; see: Toyota, K.; Yamamoto, Y.; Akiba, K. *J. Chem. Res.* **1999**, 386.

(7) Frisch, M. J.; Trucks, G. W.; Schlegel, H. B.; Scuseria, G. E.; Robb, M. A.; Cheeseman, J. R.; Montgomery, J. A., Jr.; Vreven, T.; Kudin, K. N.; Burant, J. C.; Millam, J. M.; Iyengar, S. S.; Tomasi, J.; Barone, V.; Mennucci, B.; Cossi, M.; Scalmani, G.; Rega, N.; Petersson, G. A.; Nakatsuji, H.; Hada, M.; Ehara, M.; Toyota, K.; Fukuda, R.; Hasegawa, J.; Ishida, M.; Nakajima, T.; Honda, Y.; Kitao, O.; Nakai, H.; Klene, M.; Li, X.; Knox, J. E.; Hratchian, H. P.; Cross, J. B.; Bakken, V.; Adamo, C.; Jaramillo, J.; Gomperts, R.; Stratmann, R. E.; Yazyev, O.; Austin, A. J.; Cammi, R.; Pomelli, C.; Ochterski, J. W.; Ayala, P. Y.; Morokuma, K.; Voth, G. A.; Salvador, P.; Dannenberg, J. J.; Zakrzewski, V. G.; Dapprich, S.; Daniels, A. D.; Strain, M. C.; Farkas, O.; Malick, D. K.; Rabuck, A. D.; Raghavachari, K.; Foresman, J. B.; Ortiz, J. V.; Cui, Q.; Baboul, A. G.; Clifford, S.; Cioslowski, J.; Stefanov, B. B.; Liu, G.; Liashenko, A.; Piskorz, P.; Komaromi, I.; Martin, R. L.; Fox, D. J.; Keith, T.; Al-Laham, M. A.; Peng, C. Y.; Nanayakkara, A.; Challacombe, M.; Gill, P. M. W.; Johnson, B.; Chen, W.; Wong, M. W.; Gonzalez, C.; Pople, J. A. *Gaussian 03*, revision C.02; Gaussian, Inc.: Wallingford, CT, 2004.

(8) (a) Adamo, C.; Barone, V. *J. Chem. Phys.* **1999**, *110*, 6158. (b) Perdew, J. P.; Burke, K.; Ernzerhof, M. *Phys. Rev. Lett.* **1996**, *77*, 3865. (c) Perdew, J. P.; Burke, K.; Ernzerhof, M. *Phys. Rev. Lett.* **1997**, *78*, 1396.

(9) (a) Godbout, N.; Salahub, D. R.; Andzelm, J.; Wimmer, E. *Can. J. Chem.* **1992**, *70*, 560. (b) Sosa, C.; Andzelm, J.; Elkin, B. C.; Wimmer, E.; Dobbs, K. D.; Dixon, D. A. *J. Phys. Chem.* **1992**, *96*, 6630.

(10) Andrae, D.; Haeussermann, U.; Dolg, M.; Stoll, H.; Preuss, H. *Theor. Chim. Acta* **1990**, *77*, 123.

(11) Ayala, P. Y.; Schlegel, H. B. *J. Chem. Phys.* **1997**, *107*, 375.

(12) Cramer, C. *Essentials of Computational Chemistry, Theories and Models,* 2nd ed.*;* John Wiley & Sons: New York, 2004.

(13) Reed, A. E.; Curtiss, L. A.; Weinhold, F. *Chem. Rev.* **1988**, *88*, 899.

(14) (a) Boys, S. F.; Bernardi, F. *Mol. Phys.* **1970**, *19*, 553. (b) Simon, S.; Duran, M.; Dannenberg, J. J. *J. Chem. Phys.* **1996**, *105*, 11024.

(15) Dennington, R., II; Keith, T.; Millam, J.; Eppinnett, K.; Hovell, W. L.; Gilliland, R. *GaussView*, version 3.09; Semichem, Inc.: Shawnee Mission, KS, 2003.

(16) Schaftenaar, G.; Noordik, J. H. *J. Comput.-Aided Mol. Des.* **2000**, *14*, 123.

CHART 2

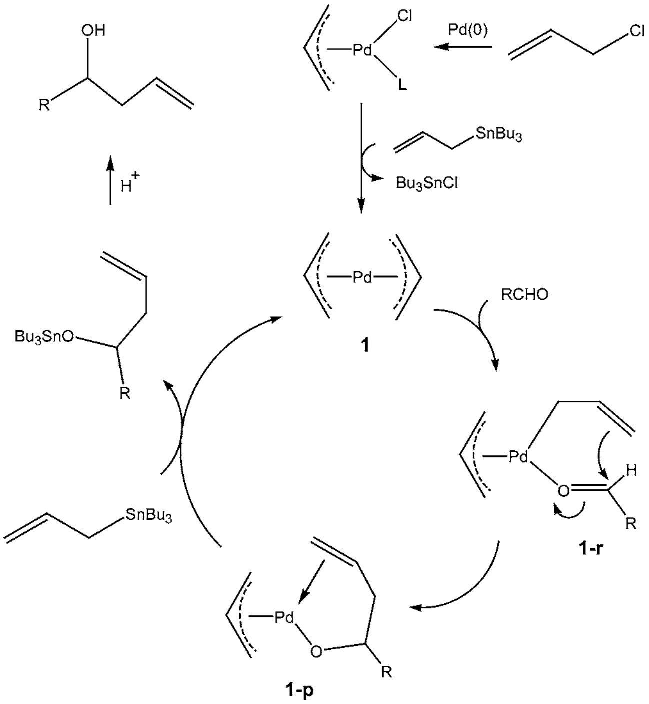

CHART 3

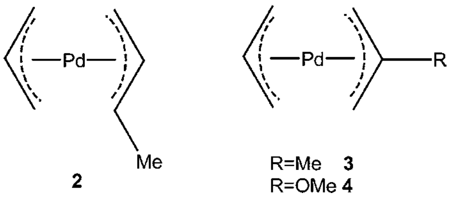

CHART 4

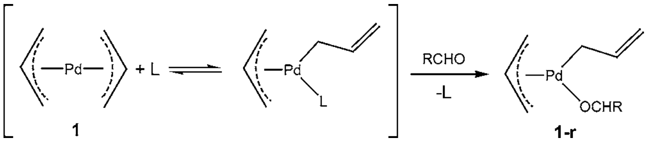

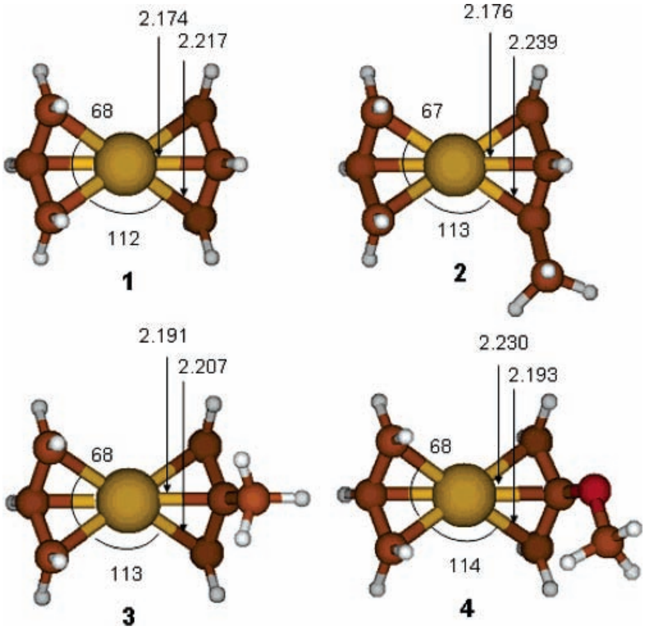

FIGURE 1. DFT-optimized structures of the symmetric bis-π-allylpalladium complex (**1**) and the mixed complexes with crotyl (**2**), methallyl (**3**), and 2-methoxyallyl (**4**) groups. Distances are given in Å, and angles are in degrees.

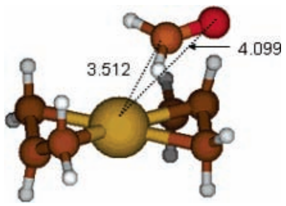

FIGURE 2. DFT-optimized structure of the **1**:CH_2O complex. Distances are given in Å.

Justification of the Theoretical Model. Adamo and Barone[8a] have analyzed the performances of the PBE1PBE hybrid functional (also termed PBE0) by computing physical properties for a number of different molecular systems. They found that this model provided molecular structures and properties with a similar and sometimes even better accuracy than that achieved by more popular hybrid functionals.

Results and Discussion

A. Bis-π-Allylpalladium Complexes. Before investigating the mechanism of the Pd(II)-catalyzed allylation of aldehydes, it is worth analyzing the molecular structures of **1** (Chart 2) and the mixed bis-π-allylpalladium complexes **2**−**4** (Chart 3) resulting from the η^3 coordination of allyl, crotyl, methallyl, and 2-methoxyallyl groups to the π-allylpalladium moiety. Figure 1 shows the optimized geometries of complexes **1**−**4**. The presence of a methyl at position 1 in the allyl group to yield crotyl has almost no effect on the length of the central Pd−C bond length, which changes from 2.174 to 2.176 Å. In contrast, the introduction of the methyl in position 2 in the coordinated allyl group to yield methallyl lengthens the Pd−C bond to 2.191 Å. Even larger than that is the lengthening provoked by the presence of OMe at position 2, which yields a central Pd−C bond length of 2.230 Å. The replacement of one π-allyl unit in **1** with crotyl, methallyl, and 2-methoxyallyl groups does not affect the geometry of the opposing π-allyl unit, whose C−Pd−C angle adopts the constant value of ~68°. Although the lack of crystallographic data for these specific complexes prevents a direct comparison with the optimized structures shown in Figure 1, a calculation performed on the bis(η^3-2-methallyl)Pd(II) complex yielded an optimized geometry which is in satisfactory agreement with the experimental structure determined by Gozum et al. (structure not shown).[17]

The natural charge of Pd in **1**−**4** corresponds to +0.61 au and is practically unaffected by the nature of the coordinated π-allyl group. The natural charges of the C atoms in the coordinated methallyl (**3**) and 2-methoxyallyl (**4**) groups maintain the (pseudo)symmetric character with respect to the plane containing Pd and the central C atoms of the ligands, as in the coordinated π-allyl groups of **1**, whereas in the crotyl group of **2**, there exists a significant concentration of negative charge on its external Me group (−0.63 au).

B. Aldehyde Coordination to Palladium. As shown in Chart 2, the first step of the catalytic cycle is concerned with the

---

[17] Gozum, J. E.; Pollina, D. M.; Jensen, J. A.; Girolami, G. S. *J. Am. Chem. Soc.* **1988**, *110*, 2688.

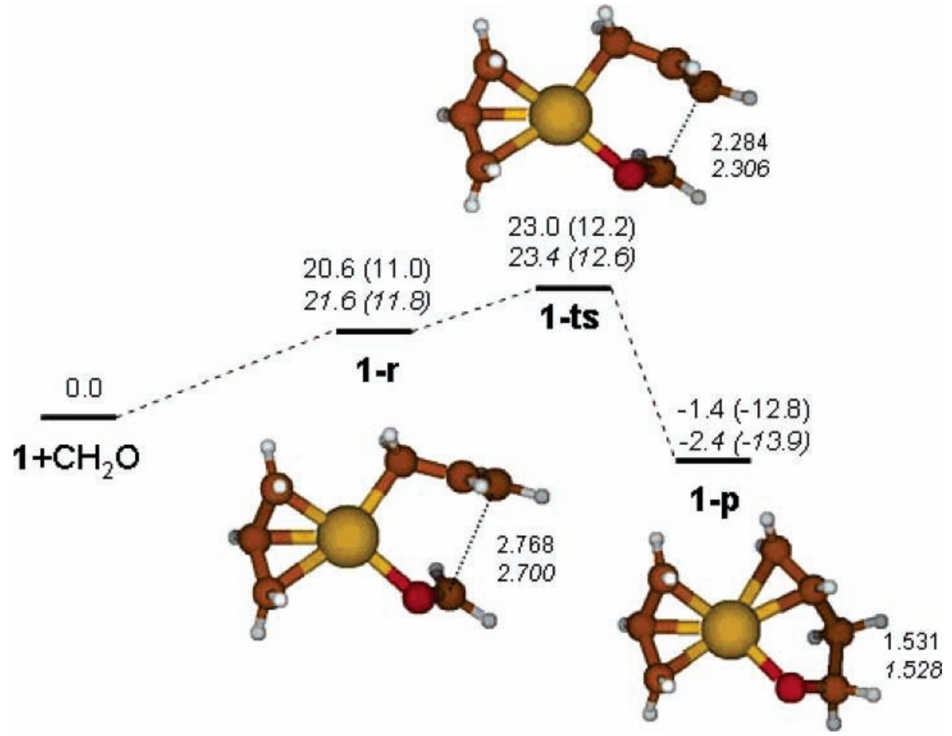

FIGURE 3. Aldehyde allylation reaction via the bis-π-allylpalladium complex **1**. The relative Gibbs free energies and ZPE-corrected electronic energies (in parentheses) are given in kcal/mol. The values in italics correspond to results obtained using the SDD basis set for Pd only. Distances are given in Å.

coordination of aldehyde to the Pd atom of the bis-π-allylpalladium complex **1** to form **1-r**. It must be noticed, however, that the aldehyde does not react directly with the bis-π-allylpalladium complex **1**. Rather, experiments[2a] suggest that the latter is likely to form an equilibrium with the (η^1-allyl)(η^3-allyl)PdL complex bearing a bulky ligand (L), such as PPh_3 or $SnBu_3$, as shown in Chart 4. The bulky ligand, L, of (η^1-allyl)(η^3-allyl)PdL can then be rapidly displaced by the aldehyde to yield complex **1-r** shown in Charts 2 and 4 (see also eq 5 and Scheme 1 in ref 2a). Our DFT calculations support this view; the interaction of CH_2O with **1** does not yield the hypothetical pentacoordinated trigonal bipyramidal (TBP) transition-state complex with the aldehyde molecule coordinated (via oxygen) to Pd in the apical position but does yield the weakly bonded complex (**1**:CH_2O) characterized by a long Pd$\cdots$O distance at 4.099 Å, as shown in Figure 2. The BSSE-corrected binding energy computed for this complex at the PBE1PBE/DGDZVP level of theory corresponds to -1.4 kcal/mol.

Further support for the above arguments was obtained by performing a series of relaxed potential energy surface (PES) scan calculations where either the Pd$\cdots$O distance of **1**:CH_2O was gradually shortened or the Pd$-$O bond of **1-r** was gradually elongated in steps of 0.2 Å. These relaxed PES scan calculations showed that the two species, **1**:CH_2O and **1-r**, are not energetically connected to each other through a common TS.

C. Transition State of the RDS. According to the mechanism proposed by Yamamoto and co-workers, the rate-determining step (RDS) of the allylation reaction involves the nucleophilic attack of an allyl C atom to the carbonyl group coordinated (via oxygen) to Pd with subsequent formation of a covalent C$-$C bond (Chart 2).[2a,b] We have investigated the geometries and energies associated with the species that are formed along this RDS with the aid of DFT calculations performed at the PBE1PBE/DGDZVP level of theory. The results are shown in Figure 3 (the results obtained using the SDD basis set for Pd only are written in italics and will be commented on later). The relative Gibbs free energy and the ZPE-corrected electronic energy (in parentheses) are calculated with respect to a standard material represented by **1** and CH_2O. As shown in this figure, coordination of the aldehyde to the Pd(II) center of **1** via the mechanism depicted in Chart 4 results in a change of coordination mode of one allyl group from η^3 to η^1. The C$\cdots$C distance in the precursor complex **1-r** corresponds to 2.768 Å. This same distance shortens to 2.284 in the TS (**1-ts**), whose associated activation Gibbs free energy ($\Delta G^{\ddagger}$) corresponds to 23.0 kcal/mol. Note that the free energy difference ($\Delta\Delta G^{\ddagger}$) between **1-ts** and **1-r** amounts to only 2.4 kcal/mol. In the product complex, **1-p**, the newly formed C$-$C bond has a length of 1.531 Å. Also, we notice that the formal double C$=$C bond of **1-p** (see also Chart 2) coordinates to the metal center through a dative-like π bond with Pd$-$C distances of 2.361 and 2.273 Å. The free energy difference (ΔG) between **1-p** and the precursor material (**1**+CH_2O) corresponds to -1.4 kcal/mol, which indicates that the reaction is thermodynamically favored (exergonic).

D. Chemoselectivity. The chemoselectivity of the aldehyde allylation reaction can be controlled when mixed bis-π-allylpalladium intermediates **2**$-$**4** (Chart 3) are being formed by reacting the Pd(II) complex with crotyl-, methallyl-, and 2-methoxyallylstannanes, respectively. Accordingly, experiments indicate that, in the case of **2**, the p-allyl group is transferred to the aldehyde, whereas in the case of **3** and **4**, the methallyl and 2-methoxyallyl groups, respectively, are transferred to the aldehyde.[2] To provide a rationale for these experiments, we have

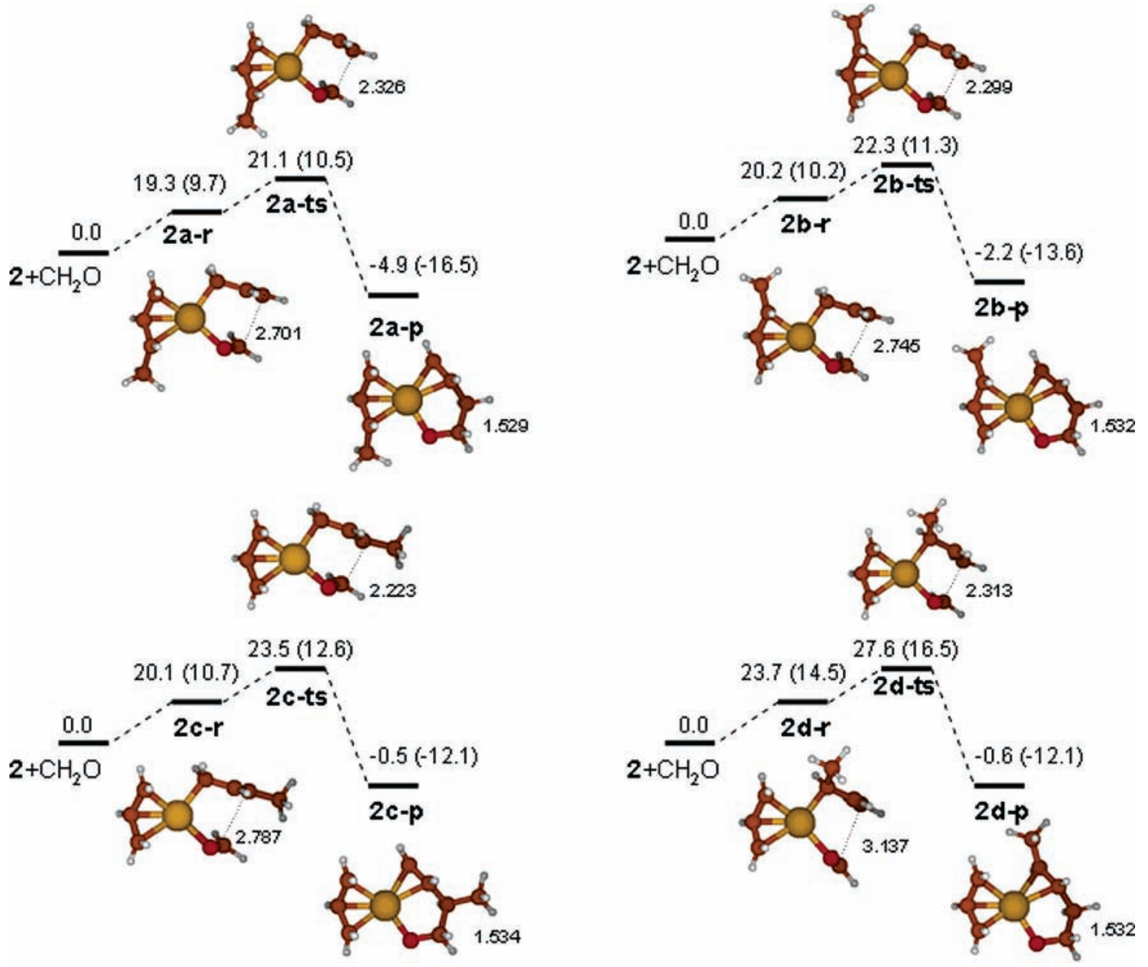

FIGURE 4. Allylation reaction via the mixed (π-crotyl, π-allyl)Pd complex **2**. The relative Gibbs free energies and ZPE-corrected electronic energies (in parentheses) are given in kcal/mol. Distances are given in Å.

TABLE 1. Computed Activation Energies Associated with the Formation of TS from the Corresponding Precursor Complex[a]

TS	$\Delta\Delta E^‡$	$\Delta\Delta(E+\text{ZPE})^‡$	$\Delta\Delta G^‡$
1-ts	0.7	1.2	2.4
1-ts	*0.4*	*0.8*	*1.8*
2a-ts	0.4	0.8	1.8
2b-ts	0.6	1.1	2.1
2c-ts	1.3	1.9	3.4
2d-ts	1.0	2.0	3.9
3a-ts	0.6	1.0	2.0
3b-ts	0.5	0.3	1.2
4a-ts	0.8	1.0	2.2
5-ts	*0.3*	*0.7*	*1.5*

[a] Values in italics correspond to calculations done using the SDD basis set[10] for the metal center only.

carried out a series of DFT calculations on the complexes that originated from the coordination of formaldehyde to **2**−**4**.

Figure 4 shows the energy barriers for the species that originated from the aldehyde allylation reaction that proceeds via the mixed (π-crotyl, π-allyl)Pd complex **2** (Chart 3). Relative Gibbs free energies and ZPE-corrected electronic energies (in parentheses) are calculated with respect to a common standard material represented by **2** and CH_2O. Four possible reaction channels have been investigated. They differ from each other in the coordination mode (η^3-type or η^1-type) and orientation of the crotyl group with respect to the coordinated aldehyde in the precursor complex. Other reaction channels resulting from sterically hindered precursor complexes, which are characterized by short Me···Pd distances, were not considered. The smaller activation free energy barrier (21.1 kcal/mol) is that arising from the TS, **2a-ts**, having the crotyl group η^3-coordinated to Pd and with the Me group oriented on the same side of the coordinated aldehyde. When the Me group is oriented on the opposite side of the coordinated aldehyde, as in **2b-ts**, the computed free energy of activation increases to 22.3 kcal/mol.

In both of the cases discussed previously, aldehyde is transferred to the allyl group. On the other hand, higher activation free energies of 23.5 and 27.6 kcal/mol are required for the transfer of aldehyde to crotyl when the latter group is η^1-coordinated to Pd, as in **2c-ts** and **2d-ts**, respectively. The large $\Delta G^‡$ barrier computed for **2d-ts** arises from the Me group of crotyl being in close spatial proximity to the Pd center (Pd···Me = 3.120 Å), which destabilizes the TS. Steric hindrance is not as severe in **2c-ts**, whose crotyl group appears to be affected by hyperconjugative effects, which affect its nucleophilic reactivity toward the coordinated aldehyde. An inspection of the natural atomic charges of the precursor complex **2c-r** indicates that the charge of the C atom involved in the formation of the C−C bond is considerably smaller than those of the other precursor complexes (−0.27 au versus −0.50 au). Notice that all four RDS's are thermodynamically favored ($\Delta G < 0$), although only two reaction channels are characterized by ΔG values that are smaller than −1 kcal/mol (see **2c-p** and **2d-p**).

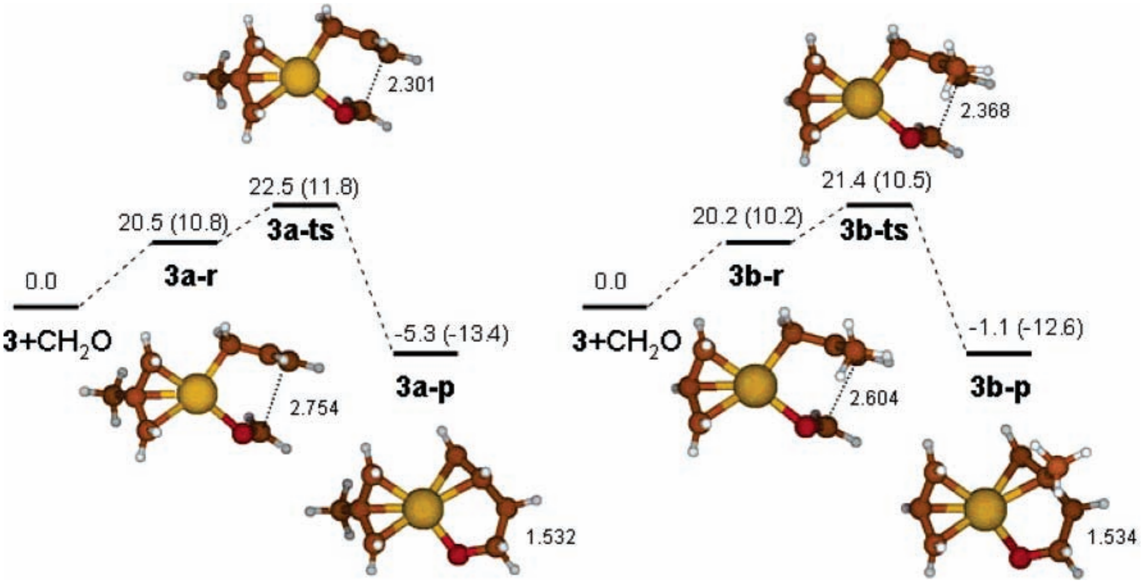

FIGURE 5. Allylation reaction via the (π-methallyl, π-allyl)Pd complex **3**. The relative Gibbs free energies and ZPE-corrected electronic energies (in parentheses) are given in kcal/mol. Distances are given in Å.

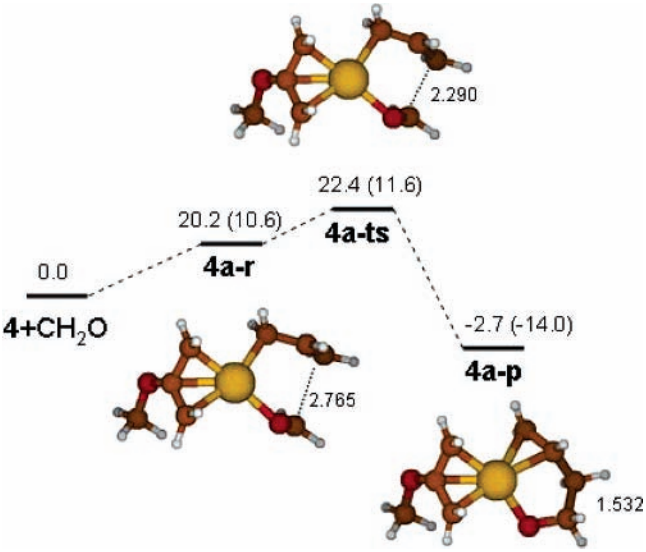

FIGURE 6. Aldehyde allylation reaction via the (π-2-methoxyallyl, π-allyl)Pd complex **4**. The relative Gibbs free energies and ZPE-corrected electronic energies (in parentheses) are given in kcal/mol. Distances are given in Å.

Overall, the present computational results indicate that, for the mixed (π-crotyl, π-allyl)Pd complex **2** (Chart 3), the aldehyde is transferred to the π-allyl group, as experimentally observed.[2a]

Table 1 reports the computed activation energies associated with the formation of a TS from the corresponding precursor complex. As it can be seen, these values are relatively small in comparison to the energy differences computed with respect to the standard material, the largest of them being ~4 kcal/mol. Nevertheless, it is worth noticing that the $\Delta\Delta G^{\ddagger}$ values of **2a-ts**, **2b-ts**, **2c-ts**, and **2d-ts** show the same energy ordering as that of the corresponding $\Delta G^{\ddagger}$ values reported in Figure 4.

Figure 5 shows the aldehyde allylation reaction that proceeds via the mixed (π-methallyl, π-allyl)Pd complex **3** (Chart 3). As shown in this figure, two precursor complexes are conceivable, one having an η^3-coordinated methallyl group (**3a-r**) and the other with the η^1-coordinated methallyl group (**3b-r**). Relative Gibbs free energies and ZPE-corrected electronic energies (in parentheses) are calculated with respect to a common standard material represented by **3** and CH$_2$O. The TS (**3b-ts**) generated from **3b-r** is characterized by an activation free energy of 21.4 kcal/mol, whereas that (**3a-ts**) generated from **3a-r** has a $\Delta G^{\ddagger}$ value of 22.5 kcal/mol. This result is in nice agreement with experiments,[2] indicating that, in the case of mixed complex **3**, the methallyl group, rather than the π-allyl group, is the one transferred to the aldehyde; the latter is a spectator.

Figure 6 shows the aldehyde allylation reaction as it proceeds through the mixed (π-2-methoxyallyl, π-allyl)Pd complex **4** (Chart 3). Here, the relative Gibbs free energies and ZPE-corrected electronic energies (in parentheses) are calculated with respect to a common standard material represented by **4** and CH$_2$O. The activation free energy of the RDS, leading to TS complex **4a-ts** with the 2-methoxyallyl group η^3-coordinated to Pd(II), corresponds to 22.4 kcal/mol. We have been unable, however, to optimize the geometry of the asymmetric precursor complex (**4b-r**) having the allyl group η^3-coordinated to Pd(II) since the optimization proceeds directly toward the product. Of the two possible product complexes shown in Figure 7, the conformer **4b-p(1)**, with the Me−O−C═C torsion angle in the syn conformation, is ~2.5 kcal/mol (ΔE+ΔZPE) more stable than **4b-p(2)**, with this same torsion angle in the anti conformation. The Gibbs free energy of the reaction leading to **4b-p(1)** corresponds to −3.2 kcal/mol, which is lower than the value of −2.7 kcal/mol calculated for **4a-p** (see Figure 6). In summary, the absence of an energy barrier (at least at the present level of theory) indicates that the 2-methoxyallyl group is the one that is likely to be transferred to the coordinated formaldehyde molecule, while the η^3-allyl group acts as a spectator, in nice agreement with experiments.[2]

E. Comparison with Szabó's Mechanism. As mentioned in the Introduction, Szabó has suggested a different mechanism of aldehyde allylation via bis-π-allylpalladium complexes.[4] Accordingly, a phosphine coordinates the metal center via the formation of a metal−phosphorus bond, whereas the aldehyde

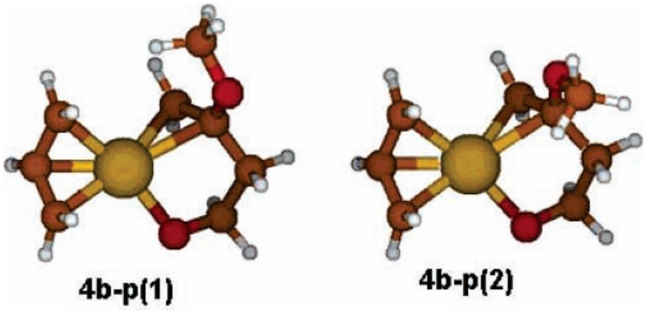

FIGURE 7. DFT-optimized structures of the product complex conformers arising from the attack of the aldehyde to the η^1-coordinated 2-methoxyallyl group.

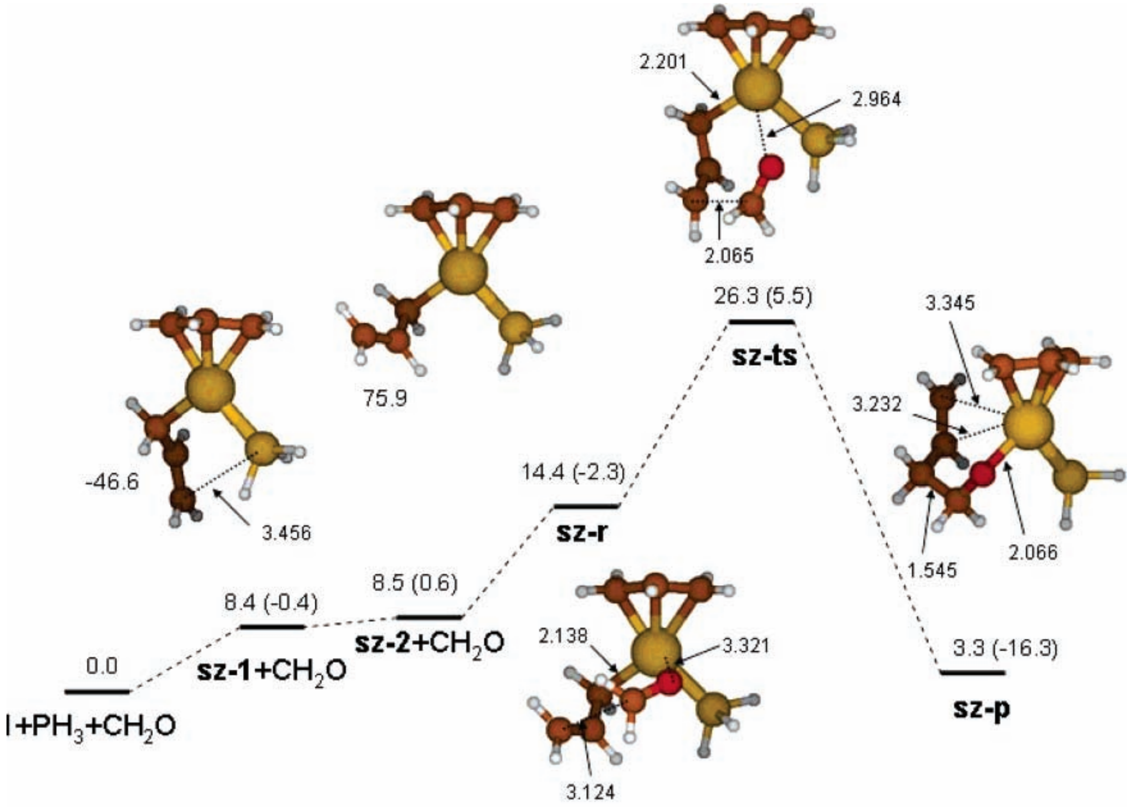

FIGURE 8. Aldehyde allylation via phosphine coordination to palladium (Szabó's mechanism). The relative Gibbs free energies and ZPE-corrected electronic energies (in parentheses) are given in kcal/mol. Distances are given in Å, and angles are given in degrees.

reacts with the η^1-coordinated allyl group while approaching the complex from the solution phase. The activation energy calculated by Szabó at the B3PW91/LANL2DZ+P level of theory corresponds to 4.3 kcal/mol (the ZPE-corrected value was 7.5 kcal/mol). Both of these energies have been computed with respect to a precursor complex (labeled **1e** in Szabó's paper) containing η^1- and η^3-coordinated allyl groups along with a phosphine ligand attached to the Pd center. It would be more correct, however, to calculate these energies with respect to a standard precursor material rather than with respect to a short-lived precursor complex. This, along with the differences in model chemistries employed by Szabó and in the present study, prompted us to reinvestigate Szabó's mechanism at the PBE1PBE/DGDZVP level of theory.

Figure 8 shows the results of our DFT calculations. To facilitate comparison, our optimized structures are oriented in a manner similar to that of the structures presented in Szabó's paper.[4] Relative Gibbs free energies and ZPE-corrected electronic energies are calculated with respect to a standard material represented by **1**, PH$_3$, and CH$_2$O. Interestingly, two conformers of the precursor complex (η^1-allyl)(η^3-allyl)Pd(PH$_3$) have been located, one (**sz-1**) with the P−Pd−C−C torsion angle at −46.6° and the other with this same torsion angle at 75.9°. Although these two conformers are characterized by similar ΔG values, namely, 8.4 kcal/mol for **sz-1** and 8.5 kcal/mol for **sz-2**, their stabilities are slightly different, as indicated by the difference in E+ZPE; **sz-1** is about 1 kcal/mol lower in energy than **sz-2**. The conformation of the former complex, however, does not allow the aldehyde molecule to approach both the terminal CH$_2$ moiety of the η^1-allyl group and the Pd center at the C···PH$_3$ distance of 3.456 Å. This result indicates that a conformational change would be necessary for **sz-1** to achieve the catalytically active conformation of **sz-2**.

When CH$_2$O approaches **sz-2** from the solution phase, a weakly bonded complex (**sz-r**) is formed. The BSSE-corrected binding energy computed for this complex corresponds to −3.2

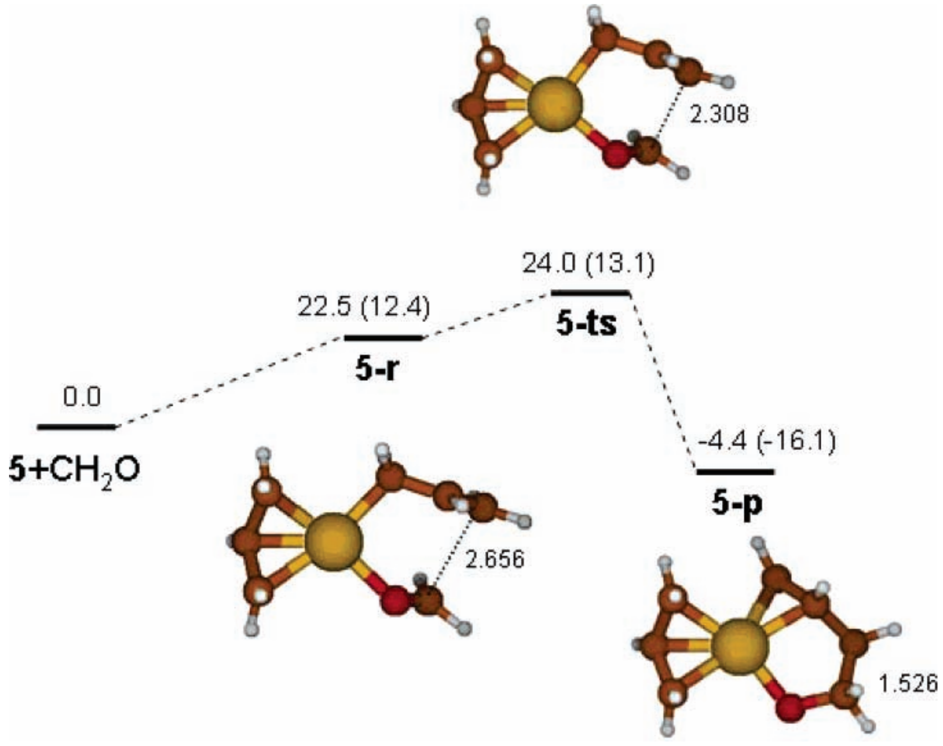

FIGURE 9. Aldehyde allylation reaction via the bis-π-allylplatinum complex. The relative Gibbs free energies and ZPE-corrected electronic energies (in parentheses) are given in kcal/mol. Distances are given in Å.

kcal/mol. This value of the binding energy is in line with the ZPE-corrected energy of **sz-r**, which is lower than that of **sz-2**+CH_2O (the relative E+ZPE value of **sz-r** is −2.3 kcal/mol, while that of **sz-2**+CH_2O is 0.6 kcal/mol). However, the relative free energy value (ΔG) computed for **sz-r** corresponds to 14.4 kcal/mol, as shown in Figure 8. The TS arising from **sz-r** and showing the formation of a C−C bond between the aldehyde and the η^1-allyl group has a relative Gibbs free energy of 26.3 kcal/mol. This value of ΔG is 3.3 kcal/mol higher than that calculated for the aldehyde allylation reaction that proceeds via **1-ts** (see Figure 3). It is interesting to notice that the relative ZPE-corrected electronic energies of **sz-ts** and **1-ts** (values given in parentheses), computed with respect to the corresponding precursor materials, show an opposite trend; the $\Delta(E$+ZPE) energy of **sz-ts** corresponds to 5.5 kcal/mol (Figure 8), while the value computed for **1-ts** is 12.2 kcal/mol (Figure 3). However, given that the rate of a reaction depends on the (Gibbs) free energy difference between starting materials and the rate-limiting TS, we conclude that the mechanism proposed by Yamamoto and co-workers (Chart 2) is favored with respect to that of Szabó. The final comment about the aldehyde allylation reaction of Figure 8 is reserved for the free energy difference between the reactants (**1**+PH_3+CH_2O) and the product (**sz-p**), which is a positive quantity, namely, $\Delta G = 3.3$ kcal/mol. This result indicates that the mechanism proposed by Szabó is endergonic, and hence, the reaction in the reverse direction would be thermodynamically favored.

F. Comparison with the Pt(II)-Catalyzed Allylation Reaction. In their original study, Yamamoto and co-workers also employed a platinum complex, namely, $PtCl_2(PPh_3)_2$, as an alternative catalyst for the allylation reaction.[2a] Interestingly, they found that, under the same reaction conditions, the Pt(II) catalyst was the best among the catalysts examined. We were much intrigued to understand the possible reasons for the origin of the better catalytic performance of the platinum catalyst against the palladium one and thus decided to explore the energetics of the Pt(II)-catalyzed allylation of formaldehyde. These calculations employed the same basis set as that used in the study of the Pd(II)-catalyzed reactions, namely, the DGDZVP basis set, except for platinum, which was treated with the Stuttgart−Dresden SDD basis set,[10] implementing relativistic effective core potentials (ECPs) for the heavy elements. With this basis set choice, the Pt atom is equipped with 18 valence electrons, whereas the physics of the remaining 60 core electrons is efficiently modeled with the ECP. The results of our DFT calculations are shown in Figure 9.

The Gibbs free energy of activation computed for the transition state **5-ts** with respect to a precursor material made of **5** and CH_2O corresponds to 24.0 kcal/mol. This value is slightly higher than the Gibbs free energy of activation of the Pd-catalyzed reaction, which corresponds to 23.4 kcal/mol, as shown in Figure 3 (values in italics). Despite the $\Delta G^\ddagger$ of the Pt-catalyzed reaction being 0.6 kcal/mol higher in energy with respect to that of the Pd-catalyzed reaction, we notice from Table 1 that the $\Delta\Delta G^\ddagger$ value of the latter (1.8 kcal/mol) is slightly larger than that of the former (1.5 kcal/mol). We suggest that this difference in $\Delta\Delta G^\ddagger$ is likely to be one of the factors at the origin of the differences in reaction kinetics experimentally observed for the aldehyde allylation reaction when these two catalysts are employed. Furthermore, we observe that the Pt(II)-catalyzed reaction is thermodynamically favored with respect to the Pd(II)-catalyzed reaction; the ΔG of the products is −4.4 kcal/mol (**5-p**) and −2.4 kcal/mol (**1-p**).

It is interesting to compare some structural features of the optimized geometries of both precursor and transition-state complexes of Pt(II) and Pd(II) (see Figures 3 and 9). As for the precursor complex, we notice that the C···C distance of the Pt(II) complex **5-r** (2.656 Å) is slightly shorter than that of the corresponding Pd(II) complex **1-r** (2.700 Å). On the other hand, the C···C distance in the TS is 2.306 Å for the Pd(II) complex **1-ts** and 2.308 Å for the Pt(II) complex **5-ts**. Hence, it appears that the structural differences in the precursor complexes, albeit small, are responsible for the observed differences in the computed $\Delta\Delta G^{\ddagger}$ energies (Table 1) and, hence, in the catalytic properties of the two catalysts.

Conclusions

In conclusion, we have investigated the mechanism of Pd(II)-catalyzed allylation of formaldehyde with the aid of the PBE1PBE hybrid DFT method. The calculations indicate that the mechanism involving the nucleophilic attack of the allyl group on the aldehyde coordinated to the Pd center is thermodynamically favored, that is, exergonic ($\Delta G = -1.4$ kcal/mol), and the computed Gibbs free energy of activation corresponds to 23.0 kcal/mol. In comparison, the free energy of activation computed at the same level of theory for Szabó's mechanism corresponds to 26.3 kcal/mol, and the overall reaction is endergonic ($\Delta G = 3.3$ kcal/mol). This result clearly indicates that the mechanism suggested by Yamamoto and co-workers is favored over that proposed by Szabó. The replacement of Pd(II) with Pt(II) slightly increases the $\Delta G^{\ddagger}$ value while decreasing the activation energy barrier, $\Delta\Delta G^{\ddagger}$, separating TS from the corresponding precursor complex. Further support for the mechanism presented herein arises from the chemoselectivity of the aldehyde allylation reaction conducted using mixed complexes (**2**−**4**), whose experimental outcome is well-reproduced by our theoretical calculations.

Acknowledgment. Financial support from the 21st century COE program "Giant Molecules and Complex Systems" is gratefully acknowledged.

Supporting Information Available: Tables containing the computed energies (*E*, ZPE, *E*+ZPE, *G*) and the DFT-optimized geometries (Cartesian coordinates) of the structures labeled in the text. This material is available free of charge via the Internet at http://pubs.acs.org.

JO061985R